JCTC Journal of Chemical Theory and Computation

Article

pubs.acs.org/JCTC

Electronic Excitations in Push–Pull Oligomers and Their Complexes with Fullerene from Many-Body Green's Functions Theory with Polarizable Embedding

Björn Baumeier,*[,†] Michael Rohlfing,[‡] and Denis Andrienko[†]

[†]Max Planck Institute for Polymer Research, Ackermannweg 10, 55128 Mainz, Germany

[‡]Institut für Festkörpertheorie, Westfälische Wilhelms-Universität Münster, Wilhelm-Klemm-Str. 10, 48149 Münster, Germany

ABSTRACT: We present a comparative study of excited states in push–pull oligomers of PCPDTBT and PSBTBT and prototypical complexes with a C_{60} acceptor using many-body Green's functions theory within the *GW* approximation and the Bethe–Salpeter equation. We analyze excitations in oligomers up to a length of 5 nm and find that for both materials the absorption energy practically saturates for structures larger than two repeat units due to the localized nature of the excitation. In the bimolecular complexes with C_{60}, the transition from Frenkel to charge transfer excitons is generally exothermic and strongly influenced by the acceptor's position and orientation. The high CT binding energy of the order of 2 eV results from the lack of an explicit molecular environment. External polarization effects are then modeled in a *GW*-BSE based QM/MM approach by embedding the donor–acceptor complex into a polarizable lattice. The lowest charge transfer exciton is energetically stabilized by about 0.5 eV, while its binding energy is reduced to about 0.3 eV. We also identify a globally unbound charge transfer state with a more delocalized hole at higher energy while still within the absorption spectrum, which opens another potential pathway for charge separation. For both PCPDTBT and PSBTBT, the energetics are largely similar with respect to absorption and the driving force to form intermediate charge transfer excitations for free charge generation. These results support that the higher power conversion efficiency observed for solar cells using PSBTBT as donor material is a result of molecular packing rather than of the electronic structure of the polymer.

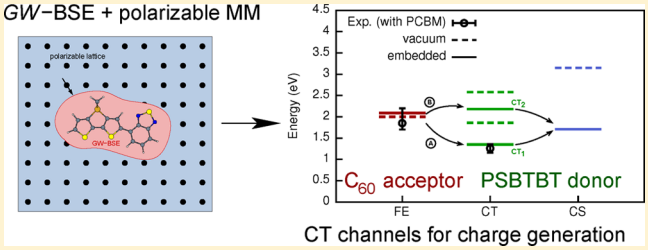

1. INTRODUCTION

Conjugated polymers are organic materials with extended π-conjugated systems, which can show metallic or semiconducting electrical properties. Among their unique characteristics is the tunability of their electronic structure by chemical synthesis and control of morphology. The additional potential of solution processing makes them attractive materials for the use in various optoelectronic devices, such as light-emitting diodes,[1−4] field effect transistors,[5−8] optically pumped lasers,[9] and organic solar cells.[10,11] Even though the modification of materials and their processing has resulted in significant improvement of organic solar cells in recent years, their record single-junction efficiencies of about 10% are still substantially lower than their thermodynamic limit,[12] which is argued to be slightly below the Shockley–Queisser limit of 31% for p–n junction solar cells.[13]

The generation of free charges after photoexcitation of the material is one of the factors influencing solar cell efficiency. Localized excitons exhibit a strong electron–hole binding energy that cannot be overcome by thermal energy alone, and donor–acceptor structures are required to split the charges. However, the actual mechanism for charge generation at the donor–acceptor interface is not fully clear. In particular, the behavior of the charge transfer (CT) excitons formed at the phase boundary is crucial for understanding the light-energy conversion process. In the literature, hot and relaxed CT state mechanisms and field-dependence, as well as the influence of delocalization, e.g., for a hole along a polymer chain, are being discussed.[14−19]

One of the unresolved issues concerns how small synthetic variations affect photovoltaic performance. PCPDTBT is a prototypical low-bandgap push–pull polymer, formed from alternating electron-rich benzothiadiazole (BT) and electron-deficient cyclopentadithiophene (CPDT) units. A silole-based derivative (PSBTBT) is realized by substitution of the bridging C atom in CPDT with Si (see chemical structures in Figure 1). As donor material in blends with PCBM as the acceptor, the silicon-based polymer shows higher solar cell efficiency.[20,21] The exact reason for this difference is unknown and could be attributed to higher crystallinity, improved charge mobility (3×10^{-4} vs 1×10^{-3} $cm^2/(Vs)$),[22] reduced bimolecular recombination, or reduced formation of charge transfer states. Separating the molecular electronic structure and morphological changes is necessary to assess the respective effects caused by the atomic substitution.

In this paper, we aim to gain microscopic insight into the nature of electronic excitations in oligomers of PCPDTBT and PSBTBT in combination with C_{60}. To this end, we employ

Received: April 3, 2014
Published: July 21, 2014

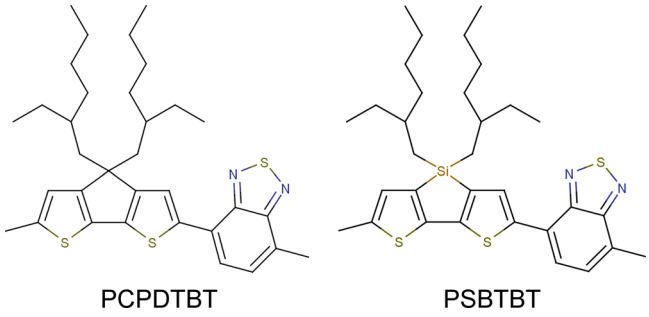

Figure 1. Chemical structures of PCPDTBT and PSBTBT.

many-body Green's functions theory[23] in the *GW* approximation with the Bethe–Salpeter equation (*GW*-BSE) to calculate excited states in these complexes. The use of *GW*-BSE for quantum chemical applications has received growing attention recently,[24−27] most notably because it accurately yields the characteristics of both localized Frenkel and bimolecular CT excitations on equal footing,[28,29] e.g., in typical small molecule-based donor–acceptor structures for organic solar cells. Here, we scrutinize the performance of *GW*-BSE for the larger push–pull polymers PCPDTBT and PSBTBT. We focus on the dependence of optically active excitations on the number of repeat units in pure oligomers and in complexes with C_{60}. We analyze the sensitivity of intermolecular CT excitons on the relative position and orientation of the donor and acceptor molecules. To model the effects of a polarizable environment, we embed the (bi)molecular complexes in a polarizable lattice and determined the respective excitations as self-consistent solutions of a hybrid quantum mechanics/molecular mechanics (QM/MM) scheme. The resulting excitation energies are in good agreement with experimental data available for PSBTBT and allow us to identify two possible routes for charge generation via different CT states.

2. METHODOLOGY

In the following, the essential ideas of many-body Green's functions theory within the *GW* approximation and the Bethe–Salpeter equation are briefly summarized. More details about the procedure and its implementation can be found in refs 25, 29, and 30. Charged (electron removal/addition) and neutral (optical) excitations are treated using many-body Green's functions theory. This approach is based on a set of Green's functions equations of motion, containing both the nonlocal, energy-dependent, electronic self-energy $\sum$ and the electron–hole interaction leading to the formation of excitons, described by the Bethe–Salpeter equation (BSE). The procedure starts with the calculation of molecular orbitals and energies on the level of density-functional theory (DFT) by solving the Kohn–Sham equations

$$\left\{-\frac{\hbar^2}{2m}\nabla^2 + V_{\mathrm{ECP}}(\mathbf{r}) + V_{\mathrm{H}}(\mathbf{r}) + V_{\mathrm{xc}}(\mathbf{r})\right\}\psi_n^{\mathrm{KS}}(\mathbf{r}) = E_n^{\mathrm{KS}}\psi_n^{\mathrm{KS}}(\mathbf{r}) \tag{1}$$

Here, V_{ECP} is an effective-core potential (ECP), V_{H} the Hartree potential, and V_{xc} the exchange-correlation potential. Single-particle excitations are then obtained within the *GW* approximation of many-body Green's functions theory, as introduced by Hedin and Lundqvist,[23] by substitution of the energy-dependent self-energy operator $\sum(\mathbf{r},\mathbf{r}',E)$ for the DFT exchange-correlation potential, giving rise to the quasi-particle equations

$$\left\{-\frac{\hbar^2}{2m}\nabla^2 + V_{\mathrm{ECP}}(\mathbf{r}) + V_{\mathrm{H}}(\mathbf{r})\right\}\psi_n^{\mathrm{QP}}(\mathbf{r}) + \int \Sigma(\mathbf{r},\mathbf{r}',E_n^{\mathrm{QP}})\psi_n^{\mathrm{QP}}(\mathbf{r}')\mathrm{d}\mathbf{r}' = E_n^{\mathrm{QP}}\psi_n^{\mathrm{QP}}(\mathbf{r}) \tag{2}$$

The self-energy operator is evaluated as

$$\Sigma(\mathbf{r},\mathbf{r}',E) = \frac{i}{2\pi}\int \mathrm{e}^{-i\omega 0^+} G(\mathbf{r},\mathbf{r}',E-\omega)W(\mathbf{r},\mathbf{r}',\omega)\mathrm{d}\omega \tag{3}$$

where

$$G(\mathbf{r},\mathbf{r}',\omega) = \sum_n \frac{\psi_n(\mathbf{r})\psi_n^*(\mathbf{r}')}{\omega - E_n + i0^+\mathrm{sgn}(E_n-\mu)} \tag{4}$$

is the one-body Green's function in quasiparticle (QP) approximation and $W = \varepsilon^{-1}v$ is the dynamically screened Coulomb interaction, comprising the dielectric function ε, computed within the random-phase approximation, and the bare Coulomb interaction v. Herein, ground-state Kohn–Sham wave functions and energies are used to determine both G and W. Since the fundamental HOMO–LUMO gap is underestimated within DFT, the self-energy and the resulting QP energies may deviate from self-consistent results. To avoid such deviations, we employ an iterative procedure, in which W is calculated only once, using a Kohn–Sham spectrum that is scissors-shifted so that the resulting QP gap is matched. Until convergence is reached, the QP energy levels are iterated, and the Green's function of eq 4 and thus the self-energy are updated. A one-shot G_0W_0 calculation from Kohn–Sham energies may differ from our results by up to several 0.1 eV. Note that our (limited) self-consistency treatment does change the QP structure of eq 4 (due to satellite structures or other consequences of a self-consistent spectral shape of $G(\omega)$).

An effective one-particle picture as the above is not sufficient to treat coupled excitations of an electron and a hole, e.g., as the result of photoexcitation. Instead, an electron–hole state can be described as

$$\Phi(\mathbf{r}_{\mathrm{e}},\mathbf{r}_{\mathrm{h}}) = \sum_{\alpha}^{\mathrm{occ}}\sum_{\beta}^{\mathrm{virt}}\left[A_{\alpha\beta}\psi_\beta(\mathbf{r}_{\mathrm{e}})\psi_\alpha^*(\mathbf{r}_{\mathrm{h}}) + B_{\alpha\beta}\psi_\alpha(\mathbf{r}_{\mathrm{e}})\psi_\beta^*(\mathbf{r}_{\mathrm{h}})\right] \tag{5}$$

where α and β denote the single-particle occupied and virtual orbitals, respectively, and $A_{\alpha\beta}$ and $B_{\alpha\beta}$ are resonant (occ → virt) and anti-resonant (virt → occ) electron–hole amplitudes. These amplitudes can be obtained by solving a non-Hermitian eigenvalue problem known as the generalized Bethe–Salpeter equation

$$\begin{pmatrix} R & C \\ -C^* & -R^* \end{pmatrix}\begin{pmatrix} A \\ B \end{pmatrix} = \Omega\begin{pmatrix} A \\ B \end{pmatrix} \tag{6}$$

in which we defined the free interlevel transition energy $D = E_{\mathrm{virt}}^{\mathrm{QP}} - E_{\mathrm{occ}}^{\mathrm{QP}}$, $R = D + \eta K^{R,x} + K^{R,d}$ is the resonant (and $-R^*$ the anti-resonant) Hamiltonian of the transition, while $C = \eta K^{C,x} + K^{C,d}$ is the coupling term between resonant and anti-resonant transitions (with $\eta = 2(0)$ for singlet (triplet) transitions). $K^{j,x}$ and $K^{j,d}$ (with $j = R,C$) are the bare exchange and screened direct terms of the electron–hole interaction kernel, respectively. We include dynamical screening effects in the electron–hole interaction kernel perturbatively (see refs 29 and

dx.doi.org/10.1021/ct500479f | J. Chem. Theory Comput. 2014, 10, 3104−3110

30 for details). Finally, Ω is the transition energy of the optical excitation.

The resonant and antiresonant parts of the full BSE (eq 6) decouple if the resonant−anti-resonant coupling terms C are much smaller than R. In this Tamm−Dancoff approximation (TDA) the electron−hole wave function is given by $\Phi_S(\mathbf{r}_e,\mathbf{r}_h) = \sum_\alpha^{occ}\sum_\beta^{virt} A_{\alpha\beta}\psi_\beta(\mathbf{r}_e)\psi_\alpha^*(\mathbf{r}_h)$, and a standard Hermitian eigenvalue problem (of smaller dimension than eq 6) needs to be solved. For typical donor molecules used in organic solar cells, we showed that the use of the TDA overestimates $\pi-\pi$ transition energies by 0.2 eV but yields the correct character of the excitations.[29]

For practical calculations according to the *GW*-BSE method, we perform single-point Kohn−Sham calculations using a modified[31] version of the Gaussian03 package,[32] PBE functional, Stuttgart−Dresden effective core potentials,[33] and associated basis sets that are augmented by additional polarization functions[34] of d symmetry. The use of ECPs offers a computational advantage as the wave functions entering the *GW* procedure are smooth close to the nuclei and do not require strongly localized basis functions, keeping the numerical effort tractable. We confirmed that the Kohn−Sham energies obtained from ECP-based calculations do not deviate significantly from all-electron results. The actual *GW*-BSE calculations are performed using a code that is specifically optimized for molecular systems.[25,29,30,35] Therein, the quantities occurring in the *GW* self-energy operator (dielectric matrix, exchange and correlation terms) and the electron−hole interaction in the BSE are expressed in terms of auxiliary atom-centered Gaussian basis functions of the form $\chi_{ijk}(\mathbf{r}) = A_{ijk}x^i y^j z^k \exp(-\alpha r^2)$. We include orbitals of s, p, d, and s^* symmetry with the decay constants α (in a.u.) 0.20, 0.67, and 3.0 for N and S, 0.25, 0.90, 3.0 for C and Si, and 0.4 and 1.5 for H atoms, yielding converged excitation energies. Note that we also confirmed that the addition of diffuse functions with decay constants smaller than 0.06 a.u. to the wave function basis set does not affect the low-lying excitations. Further technical details can be found in refs 29, 30, and 35.

3. RESULTS

3.1. Oligomer Excitations. After replacing the branched side chains shown in Figure 1 by methyl groups, ground state geometries of oligomers with one to five donor−acceptor repeat units have been optimized within DFT using the def2-TZVP basis set with the B3LYP hybrid functional. In all cases, we find stable geometries that are practically flat, with a barrier of about 25 kJ/mol between cis and trans conformations of donor and acceptor blocks. On the basis of these geometries, we evaluate the optical excitation energies within the TDA of *GW*-BSE. A total of 567 levels are used in the RPA determination of the polarizability, and two particle states are formed using the 54 highest occupied and 54 lowest virtual quasiparticle states in case of 1-mers, 1118 (107) for the 2-mers, 1669 (160) for the 3-mers, 2220 (213) for the 4-mers, and 2771 (226) for 5-mers. The resulting energies Ω of the optical active excitations are shown in Figure 2, together with the electron−hole binding energy that we estimate from the expectation value of the electron−hole interaction kernel of the Bethe−Salpeter equation $\langle K_{e-h}\rangle$. It is immediately apparent that PCPDTBT and PSBTBT show a very similar behavior; we observe a strong redshift by about 1 eV of the absorption energy from 1- to 2-mers, while it remains fairly constant for oligomers with three or more repeat units. The strong initial

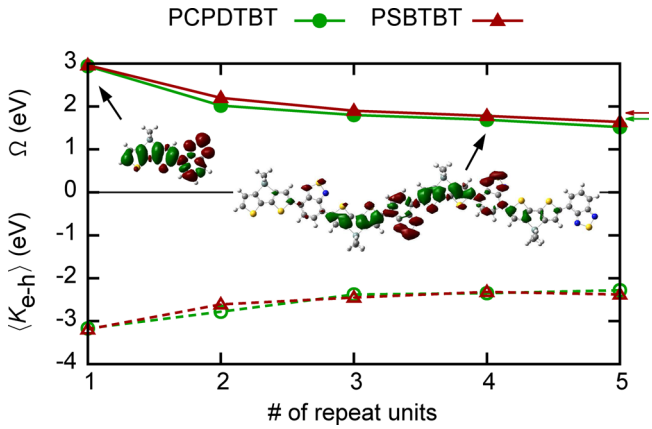

Figure 2. Excitation (Ω) and binding ($\langle K_{e-h}\rangle$) energies for oligomers of PCPDTBT and PSBTBT as a function of the number of repeat units. Arrows to the right of the graph indicate the respective energies of the absorption peak maximum in solution.[36,37]

redshift is the cumulative result of two effects related to the localization of the excitation. First, the excitation energy drops due to a quantum-size effect associated with the more delocalized nature of the excited state, which is most pronounced for the increase from one to two donor−acceptor units. Indeed, for the longer oligomers, the excitation does not delocalize over the whole molecule, but we observe a localization of the exciton on approximately three repeat units. (The slight drop in Ω for larger molecules is most likely due to DFT inaccuracies in the determination of the underlying ground state geometries.) Second, using the TDA is known to overestimate excitation energies of $\pi \rightarrow \pi^*$ transitions by several 0.1 eV for small molecules, with the effect of monotonically decreasing with size of the conjugated system. Taking resonant−anti-resonant transition coupling terms into account lowers the excitation energies by 0.2 eV for the 1-mers and 0.1 eV for 2-mers. Experimentally, the absorption spectra of the polymers have been measured in solution,[36,37] with peak energies determined to be 1.71 eV for PCPDTBT and 1.85 eV for PSBTBT, respectively. These values are also indicated by arrows on the right-hand side of Figure 2. Considering that we cannot reproduce all details of the experimental conditions, such as small solvent effects, finite temperature, or polydispersity, our calculations agree very well with the reported energies. In particular, we are able to reproduce the relative difference between PCPDTBT and PSBTBT, with the silole-based compound exhibiting roughly 0.1 eV lower excitation energies.

Mirroring the size-dependence of the excitation energies, the electron−hole binding energies shown in Figure 2 practically saturate for oligomers of three or more repeat units at a value of −2.3 eV as a result of the aforementioned characteristics of the excited states. Such high binding energies are typically obtained when excitations are calculated using molecules in vacuum[25] and are significantly modified by local electric fields and polarization effects in a molecular environment, which we will address later.

Previous studies have shown that the *GW*-BSE method yields singlet excitation energies in very good quantitative agreement with experimental data and higher order computational approaches. For instance, results for small molecules, such as silane and methane, agree within 0.1 eV with those obtained from quantum Monte Carlo and complete active space self-consistent field (CASSCF) calculations.[38] Later, similarly

convincing results have been reported for a series of biological chromophores,[35] as well as medium-sized conjugated molecules used in organic electronics.[24,29] Particularly, it has been demonstrated that *GW*-BSE can accurately describe excited states of molecules with extended π-systems as well as nonlocal excitations such as charge transfer excitations, in contrast to, e.g., time-dependent density-functional theory (TD-DFT) with commonly used functionals.[39,40] To illustrate these notions for the push−pull type oligomers at hand, we compare our *GW*-BSE results to those obtained from more routine approaches of comparable complexity as a reference. We chose configuration−interaction singles (CIS) as an example of a post Hartree−Fock method as well as TD-DFT with the B3LYP hybrid functional (TD-B3LYP) and determine the energy of the lowest optically active excitation of PSBTBT as an example using the same molecular geometries and basis sets as in the *GW*-BSE calculations.

The respective results listed in Table 1 show that CIS systematically yields higher energies (by 0.5−0.7 eV), which is mainly due to an insufficient representation of electron correlation. Excitation energies obtained with TD-B3LYP lie 0.3−0.6 eV below the ones calculated with *GW*-BSE. It should be emphasized that with our implementation *GW*-BSE is of roughly similar computational cost as CIS or TD-DFT calculations in standard packages. These notions underline the quality of the many-body Green's functions approach compared to more commonly used methods.

Table 1. Excitation Energies (in eV) of PSBTBT Oligomers As Obtained from *GW*-BSE, CIS, and TD-B3LYP Calculations

PSBTBT	1-mer	2-mer	3-mer	4-mer	5-mer
GW-BSE	2.96	2.20	1.90	1.78	1.64
CIS	3.43	2.70	2.49	2.39	2.34
TD-B3LYP	2.38	1.77	1.53	1.40	1.34

All in all, the results obtained for isolated oligomers show that it is sufficient to limit *GW*-BSE calculations on 3-mers of the oligomers to gain reliable insight into the photophysical properties of PCPDTBT and PSBTBT in combination with C_{60}.

3.2. Donor−Acceptor Complexes of 1-mers with C_{60}. We now focus on prototypical donor−acceptor complexes of PCPDTBT and PSBTBT with C_{60} by first starting out with 1-mers of the polymer material, assessing the sensitivity of the bimolecular charge transfer excitation energies on the relative positions and orientations of the electron accepting fullerene with respect to the polymer. By positioning either a pentagon (5) or hexagon (6) face above the electron-rich CPDT or SBT (*D*) and electron-deficient BT (*A*) units, we prepared four distinct initial configurations of C_{60} stacked on top of the oligomer backbone. We then optimize the respective geometries with DFT on the B3LYP/def2-TZVP level with additional van der Waals interactions[41] taken into account. The respective stable configurations we obtain are energetically very similar, with total energies within 0.16 eV of each other. For both compounds, configuration 6-*D* is the most stable due to a maximization of π−π-interactions between the two molecules. We determine the singlet excitation spectra for the different configurations with *GW*-BSE using 1827 states in the RPA and 174 occupied and virtual states in the BSE and identify the local Frenkel and bimolecular CT excitations within them. It has been shown before[25,28] that the energies of intermolecular CT excitations can be obtained with high accuracy from *GW*-BSE. The corresponding energies are summarized in Table 2.

Table 2. Excitation (Ω) and Binding ($\langle K_{e-h}\rangle$) Energies (in eV) of Frenkel and CT Excitons in PCPDTBT and PSBTBT Complexes with C_{60}

		PCPDTBT		PSBTBT	
	type	Ω	$\langle K_{e-h}\rangle$	Ω	$\langle K_{e-h}\rangle$
5-*A*	FE	2.87	−2.87	2.90	−2.90
	CT	2.45	−2.02	2.39	−2.01
5-*D*	FE	2.90	−2.94	3.00	−2.99
	CT	2.39	−2.08	2.72	−2.05
6-*A*	FE	2.82	−2.83	2.87	−2.86
	CT	2.52	−2.21	2.30	−2.33
6-*D*	FE	3.00	−2.93	2.99	−2.97
	CT	2.16	−2.43	2.32	−2.13

Compared to the isolated 1-mers, we observe a minimal redshift of the optically active FE energies by about 0.1 eV for the 5-*A* and 6-*A* configurations. This is likely due to the proximity of the electron accepting fullerene to the electron-deficient polymer building unit and the more pronounced interactions compared to the respective *D* positions. The energies of the lowest CT excitation range from 2.16 to 2.52 eV in PCPDTBT and from 2.30 to 2.72 eV in PSBTBT. For all cases considered, we find that $\Omega_{CT} < \Omega_{FE}$, i.e., a conversion from Frenkel to a charge transfer exciton is exothermic, with a reduction in binding energy between 0.5 and 0.9 eV. Again, the properties of CT excitations appear largely similar in both PCPDTBT and PSBTBT, and no substantial difference can be identified that could be relevant for the different solar cell efficiencies.

To illustrate the differences to routine techniques, we also determined the respective excitation energies of the 5-*A* configuration of PSBTBT with C_{60} from CIS and TD-B3LYP. For CIS, we observe a qualitatively different order of the excited states, with the first excitation with at least partial charge transfer character about 1.1 eV higher in energy than Ω_{FE} = 3.42 eV. TD-B3LYP, in contrast, yields Ω_{CT} = 1.61 eV compared to the FE energy of 2.39 eV, as it is known to underestimate the energies of intermolecular CT excitations.[42] Concomitantly, the FE-CT offset as calculated with TD-B3LYP is nearly twice as large as that obtained from *GW*-BSE.

3.3. Dependence on Oligomer Length. As we have concluded from the analysis in section 3.1, the absorption energy of the oligomers effectively saturates for sizes of three or more repeat units. The complexes of PCPDTBT and PSBTBT monomers with C_{60} can therefore only serve as a qualitative indicator of orientation and position dependence of charge transfer excitations. To obtain a more quantitative insight requires explicit calculations for larger oligomers. We start out from the representative 5-*A* configurations discussed in section 3.2 and extend the 1-mer to 2- and 3-mers, respectively.

As shown in the results in Table 3, the dependence of the optically active Frenkel exciton's energy on the number of repeat units is unaffected by the presence of the C_{60} molecule. The energy of the lowest CT state (CT_1) is much more affected. Extending the length of the oligomer from one to two repeat units lowers Ω_{CT} by 0.7 eV in PCPDTBT and by 0.5 eV in PSBTBT. Concomitantly, we also identify a second charge

dx.doi.org/10.1021/ct500479f | J. Chem. Theory Comput. 2014, 10, 3104−3110

Table 3. Excitation (Ω) and Binding ($\langle K_{e-h}\rangle$) Energies (in eV) for Frenkel and CT Excitons, as Well as CS States, in PCPDTBT and PSBTBT Complexes with C_{60}, for Different Numbers of Oligomer Repeat Units[a]

	PCPDTBT			PSBTBT		
	vacuum		$\varepsilon = 3$	vacuum		$\varepsilon = 3$
type	Ω	$\langle K_{e-h}\rangle$	Ω	Ω	$\langle K_{e-h}\rangle$	Ω
			1-mer			
CT_1	2.45	−2.02	1.62	2.39	−2.00	1.77
FE	2.87	−2.87	2.95	2.90	−2.90	2.97
CS	4.20		2.23	4.25		2.32
			2-mer			
CT_1	1.76	−1.95		1.88	−2.25	
FE	2.12	−2.42		2.20	−2.55	
CT_2	2.65	−1.78		2.76	−1.73	
CS	3.21			3.47		
			3-mer			
CT_1	1.71	−1.82	1.18	1.86	−2.01	1.35
FE	1.88	−2.36	1.92	2.00	−2.40	2.09
CT_2	2.44	−1.62	1.84	2.58	−1.58	2.18
CS	3.05		1.65	3.15		1.71

[a]See insets of Figure 3 for information about the molecular arrangement.

transfer state (CT_2) in both systems 0.9 eV higher in energy as shown in Figure 3. From the insets showing the electron density difference of the excitations, one can see that this second CT excitation at 2.76 eV exhibits a more delocalized hole density, which leads to a weaker electron−hole interaction. Adding a third repeat unit does not lower the CT_1 state at all, while the energy of CT_2 is further reduced by 0.2 eV due to additional delocalization. The driving force for the FE to CT_1 conversion obtained from our calculations is lowered to as little as 0.15 eV, while energy of nearly 0.6 eV needs to be found to promote the complex to the CT_2 state. Again, this holds for both PCPDTBT and PSBTBT. We also added the energy of a charge-separated (CS) state to Figure 3 and Table 3, respectively, estimated as $\Omega_{CS} = IP_D - EA_A$, i.e., the difference of the ionization potential of the isolated oligomer and the electron affinity of the isolated C_{60}. Note that this estimate based on the unperturbed excitation energies based on isolated donor and acceptor is subject to several approximations such as the neglect of mutual polarization. A significant energy difference of 1.3 or 0.6 eV from the CT_1 and CT_2 states, respectively, needs to be overcome in the considered PSBTBT:C_{60} complex according to these bimolecular values. However, this cannot truly represent the spatially separated final state in the photogeneration of charges in an organic solar cell. Additionally, calculations on isolated complexes neglect the influence of the bulk on the respective energies including local electric fields and polarization effects of the environment and can therefore not yield a quantitative description.

3.4. Polarization Effects: Lattice Embedding. It has been shown before that the most accurate approach to obtain excitation energies in a molecular aggregate is to embed the quantum-mechanically (QM) treated complex into an environment at molecular mechanics (MM) resolution.[44−47] Such a QM/MM scheme can be realized, i.e., by representing the molecules in the MM region by a set of atomic properties such as static partial charges and polarizabilities, which then interact among each other and the QM part via classical electrostatic potentials. This obviously requires the determination of an explicit morphology of the whole system at full atomistic resolution, which is a particularly challenging task for polymer−fullerene mixtures. Here, we follow a less intricate approach by embedding the oligomer−C_{60} complex into a regular lattice and assigning an isotropic polarizability α to each lattice site. More specifically, we use a lattice spacing of 2 Å and a point polarizability that reproduces a macroscopic dielectric constant of $\varepsilon_r = 3$ according to the Clausius−Mosotti relation. We adopt Thole's model[48,49] for the polarizable interactions and couple its implementation in the VOTCA package[50] to the *GW*-BSE part. Total energies of the neutral and excited complexes are then obtained as self-consistent solutions of the combined QM/MM system, with their difference defining the excitation energy in the polarizable environment. This procedure assumes that the states of interest and in particular their localization characteristics on the QM cluster are easily identifiable. Typically, this can be expected to be the case for the Frenkel and low-energy CT excitons, on which we focus in the following.

As shown for the resulting energies of the complexes of 1-mers with C_{60} given in Table 3, the polarizable environment only has a minor effect on the energetics of Frenkel exciton because the internal charge distribution is only moderately changed during the excitation. By promoting one electron from

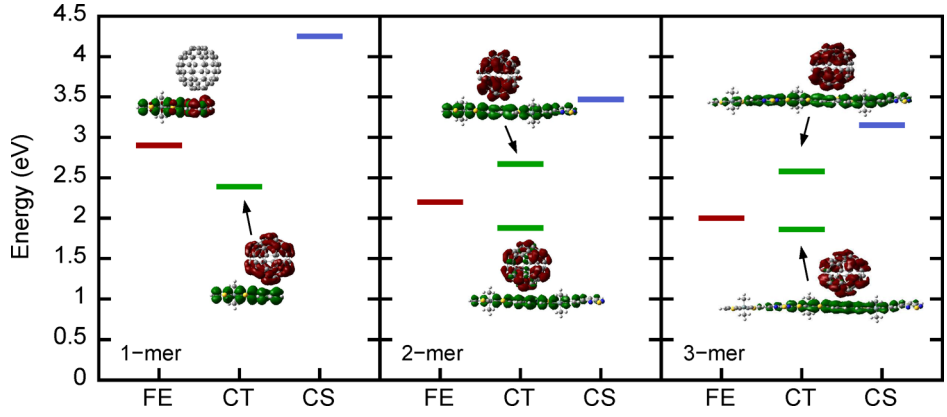

Figure 3. Energies of Frenkel and charge transfer excitations in prototypical complexes of PSBTBT and C_{60} for one, two, and three repeat units of the polymer. Insets show the respective difference electron density distribution (green: hole; red: electron) for an isovalue of $\pm 4.10^{-4}$ e/Å^3. The energy of the charge-separated state is estimated as $\Omega_{CS} = IP_D - EA_A$.

dx.doi.org/10.1021/ct500479f | J. Chem. Theory Comput. 2014, 10, 3104−3110

the oligomer to the C_{60}, the charge distribution in the CT excitation is significantly different to the one of the ground state, and we observe a significant energy stabilization by 0.83 eV in PCPDTBT and 0.62 eV in PSBTBT.

For a more quantitative situation, we consider the polarization effects on the relative energies in complexes of 3-mers with C_{60} (Table 3). The results for PSBTBT are also shown in Figure 3, together with experimental data.[37,43] The asymmetric error bars for the FE energy represent the half-width of the experimentally observed absorption peak. Again, Ω_{FE} is hardly influenced by the presence of the polarizable environment and remains very close to the measured data. The CT_1 state, in contrast, is stabilized by 0.51 eV from 1.86 to 1.35 eV. This final energy is in good agreement with value of 1.26 eV reported from the experiment.[43] As a consequence of the stronger delocalization of the hole over the oligomer, the stabilization of CT_2 is weaker, amounting to 0.40 eV, leading to a final energy of 2.18 eV. Similarly, we estimated the energy of the charge-separated state to be 1.7 eV.

The energy diagram as in Figure 4 highlights two consequences of the polarizable environment. First, the

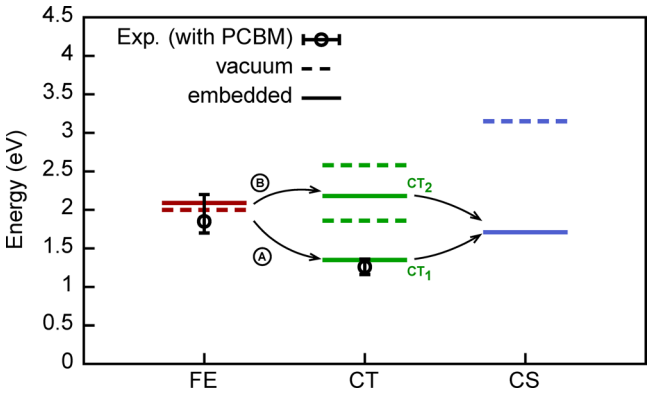

Figure 4. Energies of Frenkel and charge transfer excitations, as well as charge-separated states in the complex of a PSBTBT 3-mer and C_{60} in vacuum (dashed) and embedded in a polarizable lattice (solid) resulting from our *GW*-BSE calculations together with experimental data.[43] Arrows indicate the two possible CT-mediated channels for charge separation: **A** via the low-energy CT_1 state or **B** via the less-bound CT_2.

stabilization of CT_1 leads to an increase in the driving force for FE to CT conversion to 0.65 eV. To generate free charges via this low-energy CT pathway labeled **A** in Figure 4, one needs to overcome the energy difference of 0.36 eV according to our calculations, which may be achieved with the excess energy of the FE → CT_1 conversion. Mounting experimental and theoretical evidence points to the important role that high-energy (hot) charge transfer states play in the dissociation of Frenkel excitons at a donor−acceptor interface.[16−18] Interestingly, the results of our polarized calculations also indicate the existence of a second pathway, labeled **B** in Figure 4, via the CT_2 exciton. Its energy is close to Ω_{FE} and, taking the broadness of the absorption peak into account, a transition from FE to CT_2 appears energetically possible. In this case, the conversion to the charge-separated state could even be exothermic, i.e., pathway **B** occurs via a globally unbound CT state. We see from the data in Table 3 that a very similar situation is found in embedded PCPDTBT, with CT_2 even slightly below the FE energy. While it is possible to identify two potential pathways for the dissociation of a coupled electron−hole pair into free charges from our embedded *GW*-BSE calculations for excited states energy levels, it is difficult to draw any definite conclusion regarding which of these pathways will be preferred. For a quantitative estimate of transition rates for the cascade from FE to the charge-separated state via any of the CT excitons, it is important add explicit morphological detail beyond a single cluster representation, e.g., by means of molecular dynamics simulations of donor−acceptor interface. Such simulations account for distributions of both Ω_{FE} and the Ω_{CT} and, most importantly, yield a more realistic estimate of the final charge-separated state(s) relevant for the solar cell functionality.

4. SUMMARY

To summarize, we have presented a comparative theoretical study of electronically excited states in oligomers of PCPDTBT and PSBTBT and their complexes with C_{60}. Using many-body Green's functions theory within the *GW* approximation and the Bethe−Salpeter equation, we demonstrate that the optically active excitation is localized over no more than three repeat units and obtain absorption energies in good agreement with experimental data. Bimolecular charge transfer excitations in prototypical complexes depend sensitively on the mutual arrangement of the two molecules but do result in lower energy than the Frenkel exciton for all investigated π-stacked arrangements. By embedding large complexes in a polarizable lattice and solving the coupled QM/MM system, we approximate the effect of a molecular environment on the excitation energies, obtaining a good agreement of both Frenkel and charge transfer excitons with available experimental data. The occurrence of a second charge transfer excitation with a more delocalized hole creates the possibility of a second pathway for charge generation in both PCPDTBT and PSBTBT. All in all, the electronic excitations are very similar for both polymers, supporting the notion that different efficiencies in organic solar cells are a result of different morphological orders.

AUTHOR INFORMATION

Corresponding Author

*E-mail: baumeier@mpip-mainz.mpg.de.

Notes

The authors declare no competing financial interest.

ACKNOWLEDGMENTS

This work was partially supported by Deutsche Forschungsgemeinschaft (DFG) under the Priority Program "Elementary Processes of Organic Photovoltaics" (SPP 1355), BMBF grant MESOMERIE, and DFG program IRTG 1404. We are grateful to Tristan Bereau, Carl Poelking, and Anton Melnyk for critical reading of the manuscript. This work involved several people and no Ph.D. student.

REFERENCES

(1) Burroughes, J. H.; Bradley, D. D. C.; Brown, A. R.; Marks, R. N.; Mackay, K.; Friend, R. H.; Burns, P. L.; Holmes, A. B. *Nature* **1990**, *347*, 539−541.
(2) Braun, D.; Heeger, A. J. *Appl. Phys. Lett.* **1991**, *58*, 1982−1984.
(3) Greenham, N. C.; Moratti, S. C.; Bradley, D. D. C.; Friend, R. H.; Holmes, A. B. *Nature* **1993**, *365*, 628−630.
(4) Tessler, N.; Harrison, N. T.; Friend, R. H. *Adv. Mater.* **1998**, *10*, 64−68.

(5) Yang, Y.; Heeger, A. J. *Nature* **1994**, *372*, 344−346.
(6) Garnier, F.; Hajlaoui, R.; Yassar, A.; Srivastava, P. *Science* **1994**, *265*, 1684−1686.
(7) Sirringhaus, H.; Tessler, N.; Friend, R. H. *Science* **1998**, *280*, 1741−1744.
(8) Kawase, T.; Sirringhaus, H.; Friend, R. H.; Shimoda, T. *Adv. Mater.* **2001**, *13*, 1601−1605.
(9) McGehee, M. D.; Heeger, A. J. *Adv. Mater.* **2000**, *12*, 1655−1668.
(10) Shaheen, S.; Ginley, D.; Jabbour, G. *MRS Bull.* **2005**, *30*, 10−19.
(11) Brabec, C. J.; Gowrisanker, S.; Halls, J. J. M.; Laird, D.; Jia, S.; Williams, S. P. *Adv. Mater.* **2010**, *22*, 3839−3856.
(12) Gruber, M.; Wagner, J.; Klein, K.; Hörmann, U.; Opitz, A.; Stutzmann, M.; Brütting, W. *Adv. Energy Mater.* **2012**, *2*, 1100−1108.
(13) Shockley, W.; Queisser, H. J. *J. Appl. Phys.* **1961**, *32*, 510−519.
(14) Grzegorczyk, W. J.; Savenije, T. J.; Dykstra, T. E.; Piris, J.; Schins, J. M.; Siebbeles, L. D. *J. Phys. Chem. C* **2010**, *114*, 5182−5186.
(15) Bakulin, A. A.; Rao, A.; Pavelyev, V. G.; van Loosdrecht, P. H. M.; Pshenichnikov, M. S.; Niedzialek, D.; Cornil, J.; Beljonne, D.; Friend, R. H. *Science* **2012**, *335*, 1340−1344.
(16) Caruso, D.; Troisi, A. *Proc. Natl. Acad. Sci. U.S.A.* **2012**, *109*, 13498−13502.
(17) Troisi, A. *Faraday Discuss.* **2013**, *163*, 377−392.
(18) Jailaubekov, A. E.; Willard, A. P.; Tritsch, J. R.; Chan, W.-L.; Sai, N.; Gearba, R.; Kaake, L. G.; Williams, K. J.; Leung, K.; Rossky, P. J.; Zhu, X.-Y. *Nat. Mater.* **2013**, *12*, 66−73.
(19) Vandewal, K.; et al. *Nat. Mater.* **2014**, *13*, 63−68.
(20) Peet, J.; Kim, J. Y.; Coates, N. E.; Ma, W. L.; Moses, D.; Heeger, A. J.; Bazan, G. C. *Nat. Mater.* **2007**, *6*, 497−500.
(21) Hou, J.; Chen, H.-Y.; Zhang, S.; Li, G.; Yang, Y. *J. Am. Chem. Soc.* **2008**, *130*, 16144−16145.
(22) Scharber, M. C.; Koppe, M.; Gao, J.; Cordella, F.; Loi, M. A.; Denk, P.; Morana, M.; Egelhaaf, H.-J.; Forberich, K.; Dennler, G.; Gaudiana, R.; Waller, D.; Zhu, Z.; Shi, X.; Brabec, C. J. *Adv. Mater.* **2010**, *22*, 367−370.
(23) Hedin, L.; Lundqvist, S. *Solid State Physics: Advances in Research and Application*; Academic Press: New York, 1969; Vol. *23*; pp 1−181.
(24) Blase, X.; Attaccalite, C.; Olevano, V. *Phys. Rev. B* **2011**, *83*, 115103.
(25) Baumeier, B.; Andrienko, D.; Rohlfing, M. *J. Chem. Theory. Comput.* **2012**, *8*, 2790−2795.
(26) Marom, N.; Caruso, F.; Ren, X.; Hofmann, O. T.; Körzdörfer, T.; Chelikowsky, J. R.; Rubio, A.; Scheffler, M.; Rinke, P. *Phys. Rev. B* **2012**, *86*, 245127.
(27) van Setten, M. J.; Weigend, F.; Evers, F. *J. Chem. Theory. Comput.* **2013**, *9*, 232−246.
(28) Blase, X.; Attaccalite, C. *Appl. Phys. Lett.* **2011**, *99*, 171909.
(29) Baumeier, B.; Andrienko, D.; Ma, Y.; Rohlfing, M. *J. Chem. Theory Comput.* **2012**, *8*, 997−1002.
(30) Ma, Y.; Rohlfing, M.; Molteni, C. *Phys. Rev. B* **2009**, *80*, 241405.
(31) The source code of Gaussian03 was modified to output the matrix elements of the exchange-correlation potential in the atomic orbital basis needed to calculate the matrix $\langle n|V_{xc}|m\rangle$, where $|n\rangle$ and $|m\rangle$ are Kohn−Sham wave functions, as input for the GW-BSE steps.
(32) Frisch, M. J.; Trucks, G. W.; Schlegel, H. B.; Scuseria, G. E.; Robb, M. A.; Cheeseman, J. R.; Montgomery, J. A., Jr.; Vreven, T.; Kudin, K. N.; Burant, J. C.; Millam, J. M.; Iyengar, S. S.; Tomasi, J.; Barone, V.; Mennucci, B.; Cossi, M.; Scalmani, G.; Rega, N.; Petersson, G. A.; Nakatsuji, H.; Hada, M.; Ehara, M.; Toyota, K.; Fukuda, R.; Hasegawa, J.; Ishida, M.; Nakajima, T.; Honda, Y.; Kitao, O.; Nakai, H.; Klene, M.; Li, X.; Knox, J. E.; Hratchian, H. P.; Cross, J. B.; Bakken, V.; Adamo, C.; Jaramillo, J.; Gomperts, R.; Stratmann, R. E.; Yazyev, O.; Austin, A. J.; Cammi, R.; Pomelli, C.; Ochterski, J. W.; Ayala, P. Y.; Morokuma, K.; Voth, G. A.; Salvador, P.; Dannenberg, J. J.; Zakrzewski, V. G.; Dapprich, S.; Daniels, A. D.; Strain, M. C.; Farkas, O.; Malick, D. K.; Rabuck, A. D.; Raghavachari, K.; Foresman, J. B.; Ortiz, J. V.; Cui, Q.; Baboul, A. G.; Clifford, S.; Cioslowski, J.; Stefanov, B. B.; Liu, G.; Liashenko, A.; Piskorz, P.; Komaromi, I.; Martin, R. L.; Fox, D. J.; Keith, T.; Al-Laham, M. A.; Peng, C. Y.; Nanayakkara, A.; Challacombe, M.; Gill, P. M. W.; Johnson, B.; Chen, W.; Wong, M. W.; Gonzalez, C.; Pople, J. A. *Gaussian 03, Revision B. 05.*; Gaussian, Inc.: Wallingford, CT, 2004.
(33) Bergner, A.; Dolg, M.; Küchle, W.; Stoll, H.; Preuß, H. *Mol. Phys.* **1993**, *80*, 1431−1441.
(34) Krishnan, R.; Binkley, J. S.; Seeger, R.; Pople, J. A. *J. Chem. Phys.* **1980**, *72*, 650.
(35) Ma, Y.; Rohlfing, M.; Molteni, C. *J. Chem. Theory. Comput.* **2010**, *6*, 257−265.
(36) Fazzi, D.; Grancini, G.; Maiuri, M.; Brida, D.; Cerullo, G.; Lanzani, G. *Phys. Chem. Chem. Phys.* **2012**, *14*, 6367−6374.
(37) Chen, H.-Y.; Hou, J.; Hayden, A. E.; Yang, H.; Houk, K. N.; Yang, Y. *Adv. Mater.* **2010**, *22*, 371.
(38) Grossman, J. C.; Rohlfing, M.; Mitas, L.; Louie, S. G.; Cohen, M. L. *Phys. Rev. Lett.* **2001**, *86*, 472−475.
(39) Cai, Z.-L.; Sendt, K.; Reimers, J. R. *J. Chem. Phys.* **2002**, *117*, 5543.
(40) Dreuw, A.; Head-Gordon, M. *J. Am. Chem. Soc.* **2004**, *126*, 4007−4016.
(41) Grimme, S. *J. Comput. Chem.* **2006**, *27*, 1787−1799.
(42) Stein, T.; Kronik, L.; Baer, R. *J. Am. Chem. Soc.* **2009**, *131*, 2818−2820.
(43) Albrecht, S.; Vandewal, K.; Tumbleston, J. R.; Fischer, F. S. U.; Douglas, J. D.; Fréchet, J. M. J.; Ludwigs, S.; Ade, H.; Salleo, A.; Neher, D. *Adv. Mater.* **2014**, *26*, 2533.
(44) Risko, C.; McGehee, M. D.; Bredas, J.-L. *Chemical Science* **2011**, *2*, 1200.
(45) May, F.; Baumeier, B.; Lennartz, C.; Andrienko, D. *Phys. Rev. Lett.* **2012**, *109*, 136401.
(46) Lunkenheimer, B.; Köhn, A. *J. Chem. Theory. Comput.* **2013**, *9*, 977−994.
(47) Schwabe, T.; Sneskov, K.; Haugaard Olsen, J. M.; Kongsted, J.; Christiansen, O.; Hättig, C. *J. Chem. Theory. Comput.* **2012**, *8*, 3274−3283.
(48) Thole, B. *Chem. Phys.* **1981**, *59*, 341−350.
(49) van Duijnen, P. T.; Swart, M. *J. Phys. Chem. A* **1998**, *102*, 2399−2407.
(50) Rühle, V.; Lukyanov, A.; May, F.; Schrader, M.; Vehoff, T.; Kirkpatrick, J.; Baumeier, B.; Andrienko, D. *J. Chem. Theory. Comput.* **2011**, *7*, 3335−3345.